INTERFACE

rsif.royalsocietypublishing.org

Research

Cite this article: Ball R, Brindley J. 2015 The life story of hydrogen peroxide II: a periodic pH and thermochemical drive for the RNA world. *J. R. Soc. Interface* **12**: 20150366.
http://dx.doi.org/10.1098/rsif.2015.0366

Received: 23 April 2015
Accepted: 1 July 2015

Subject Areas:
astrobiology, chemical biology, chemical engineering

Keywords:
RNA world, hydrogen peroxide, pH oscillator, thermochemical oscillator, pH gradients, origin of life

Author for correspondence:
Rowena Ball
e-mail: rowena.ball@anu.edu.au

The life story of hydrogen peroxide II: a periodic pH and thermochemical drive for the RNA world

Rowena Ball[1] and John Brindley[2]

[1]Mathematical Sciences Institute and Research School of Chemistry, The Australian National University, Canberra 2602, Australia
[2]School of Mathematics, University of Leeds, Leeds LS2 9JT, UK

RB, 0000-0002-3551-3012

It is now accepted that primordial non-cellular RNA communities must have been subject to a periodic drive in order to replicate and prosper. We have proposed the oxidation of thiosulfate by hydrogen peroxide as this drive. This reaction system behaves as (i) a thermochemical *and* (ii) a pH oscillator, and in this work, we unify (i) and (ii) for the first time. We report thermally self-consistent, dynamical simulations in which the system transitions smoothly from nearly isothermal pH to fully developed thermo-pH oscillatory regimes. We use this oscillator to drive simulated replication of a 39-bp RNA species. Production of replicated duplex under thermo-pH drive was significantly enhanced compared with that under purely thermochemical drive, effectively allowing longer strands to replicate. Longer strands are fitter, with more potential to evolve enzyme activity and resist degradation. We affirm that concern over the alleged toxicity of hydrogen peroxide to life is largely misplaced in the current context, we survey its occurrence in the solar system to motivate its inclusion as a biosignature in the search for life on other worlds and highlight that pH oscillations in a spatially extended, bounded system manifest as the fundamental driving force of life: a proton gradient.

1. Introduction

The story of the relationship between hydrogen peroxide and life is complex and dynamic, and fraught with certain natural tensions which have led to human misapprehensions. In this work, we show that the association may be extremely ancient, that the story may have begun more than 3.7 billion years ago, the first chapter providing the periodic pH and thermal drive that enabled the RNA world to replicate, evolve and develop enzyme activity. This paper is concerned with the chemical interactions of this small, energetic molecule with the RNA world. In a companion paper [1], we examine its structure and show how its chirality may have led to the homochirality of the biological nucleic acids.

Living cells make and break hydrogen peroxide and, after a long period of misunderstanding when it was reviled as a toxic cell vandal and saboteur of gene transcription fidelity, evidence is mounting that its relationship with living organisms is intimate and vital. Metabolically produced hydrogen peroxide is now known to be essential to intracellular redox switching, and it performs important roles in processes such as circadian rhythms, insulin functioning, cell differentiation and tissue repair [2]. This relationship is usually assumed to have begun with the coevolution around 2.3 billion years ago of oxygen-evolving photosynthesis, aerobic respiration that uses oxygen as electron acceptor and enzymes for disabling the reactive oxygen species (ROS) by-products: superoxide ion, hydroxyl radical and hydrogen peroxide [3].

Yet non-biologically produced hydrogen peroxide existed in the environment before the first photosynthetic organisms appeared, and primitive anaerobes must have come to some arrangement with it [4]. And what of its role with respect to pre- and proto-cellular life, the putative RNA world? From various lines of

THE ROYAL SOCIETY PUBLISHING

evidence, to be discussed presently, we have been led to the hypothesis that the dependence of life on hydrogen peroxide is far more ancient than 'the great oxygenation event', and that this deceptively simple, seemingly plebeian, substance was the agent that enabled the very first non-cellular, self-replicating and evolving systems of the RNA world.

The RNA world hypothesis for the origin of life is well supported [5], although there are several major questions with it that have been regarded by its opponents as fatal flaws and by its proponents as problems that will be resolved by modelling and experiment. One such question concerns the necessity for thermal cycling, in the non- or proto-cellular milieu, to separate double-stranded RNA into single-stranded templates for replication, and the erstwhile lack of any realistic mechanism for it was acknowledged as a frustrating roadblock for advancement of the hypothesis [6–8]. A second concern has been the 'survival of the shortest' concept, deriving from the work of Mills *et al.* [9], which casts doubts on the 'fitness', and hence evolutionary survival, of the longer oligonucleotides essential for the development of enzyme functionality. However, in an important work, Kreysing *et al.* [10] have demonstrated experimentally a thermophoretic mechanism whereby longer nucleotide chains (more than 75 bp) were very sharply selected for and were replicated and amplified more efficiently (faster) than short chains (less than 33 bp). They also found that sustained thermal cycling in a flow-through open system is essential to this process of selecting and amplifying long chains. Their results strongly support our thesis that the RNA world must have been coupled tightly to an open, dynamic, thermally cycling environment.

In our previous work [11] (which foreshadows the current work), we proposed and tested a realistic mechanism for thermal cycling in the RNA world: we simulated a non-equilibrium flow system in which replication of a 39-bp RNA duplex was driven by thermochemical oscillations arising from an exothermic hydrogen peroxide reaction, and found that rapid amplification of the RNA occurred. Although these results await experimental verification, they are the first intimation that hydrogen peroxide may have been involved at the very dawn of pre-cellular life.

In this paper, we are concerned with the effects on RNA replication of pH oscillations, concurrently with the thermochemical oscillations considered in [11]. The reaction used in that work to provide a periodic thermal drive is the oxidation of thiosulfate ion by hydrogen peroxide, a thermochemical oscillator that has been well characterized, mostly in chemical engineering contexts [12–15]. This set of reactions is also a well-known pH oscillator, which has been studied experimentally, almost always under isothermal conditions and mostly by chemists, since the 1980s [16–23], when broad interest in chemical oscillators and pattern formation arose [24]. For conciseness, we will refer to it as the THP (thiosulfate–hydrogen peroxide) oscillator or system.

Although widely studied, thermochemical and pH oscillators, despite their obvious potential, rarely have been credited with any useful purpose other than to control simple switching operations. Liedl *et al.* [25,26] used the pH oscillator set-up by oxidation of sulfite and thiosulfate to switch a DNA structure between two conformations. Qi *et al.* [27] used the iodate–thiosulfate–ferrocyanide oscillatory pH system to drive switchable DNA machines. Our current and previous [11] works make the first suggestion we know

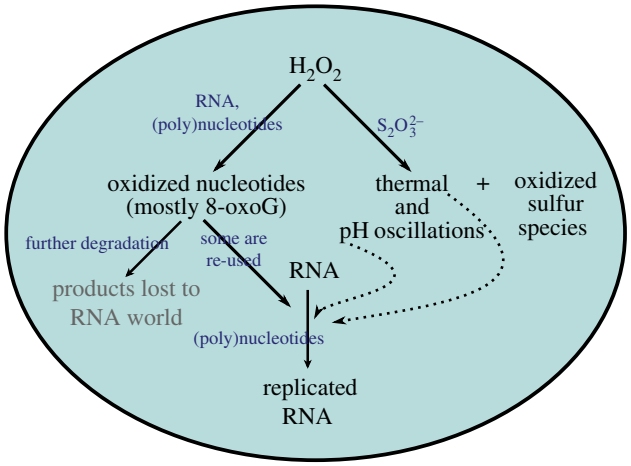

Figure 1. Hydrogen peroxide interacts with the RNA world directly (solid arrows), through oxidation of nucleotides, and indirectly (dotted arrows), by providing a periodic thermal and pH drive. (Online version in colour.)

of that nature may have made use of chemical oscillators to perform work to drive replication and metabolic processes.

In this paper, we unify, smoothly and self-consistently, the periodic behaviour of the THP system with respect to the pH and the temperature. We report results that support our hypothesis that the THP oscillator may have provided or promoted, in addition to thermal cycling, other precious functions and processes essential for replication and evolution in the RNA world:

— replication of longer RNA species is enabled; this is highly advantageous because there is considerably more scope for longer RNA chains to develop and diversify enzyme activity; and
— provision of a proton motive force: In a spatially extended, bounded system, the THP pH oscillations manifest as travelling waves and patterns, the gradients of which may have driven primitive metabolic processes in the non-cellular RNA world.

The proposed dual influence of hydrogen peroxide in the RNA world is cartooned in broadbrush in figure 1. It can interact with the RNA world directly and indirectly.

In direct interaction, as illustrated, thiosulfate ions and oxidizable sites on RNA and nucleotide species can be regarded conceptually as competing species that react with hydrogen peroxide (or its ionic or free radical dissociation products) directly. It is an unequal competition because the oxidation of thiosulfate is faster, so most of the hydrogen peroxide is consumed by that route, and damage to RNA and nucleotides is variable and patchy. Some of the oxidized nucleotides may still be usable in the RNA world, but are likely mis-paired during replication, providing a mechanism for natural selection and evolution.

Figure 1 also illustrates the indirect influence of hydrogen peroxide. The exothermic thiosulfate reaction sets up a dynamic, non-equilibrium physical environment, characterized by fluctuating temperature and pH. In effect, the RNA world is driven by the enthalpy of the peroxide O–O bond. Of course, the energy source for forging the peroxide bond is (presumably) solar or geothermal, but those sources acting directly on the RNA world cannot provide the periodic drive that is vital for sustaining and evolving a non-cellular living

system. The periodic variations in temperature and pH that result from thiosulfate oxidation feed back on the RNA world, as indicated by the dotted lines. An upswing in temperature at low pH separates double-stranded RNA, a cooling phase at higher pH favours folding of strands and complementary base or strand pairing.

In §2, we present the reactions involved in the THP oscillator, tabulate the kinetic and thermochemical data for them, and describe the dynamical model we used to simulate the THP system numerically. Results are presented in §3. In §3.1, we familiarize ourselves and the reader with the behaviour of the THP system over relevant parameter space. In §3.2, we present and discuss the outputs of simulations where the THP oscillator is used to drive RNA replication. Section 4 contains further discussions of the potential importance of hydrogen peroxide in the RNA world, and evidence of its ubiquitous occurrence in the Universe, and we summarize the achievements of this work in §5 and conclude with an imprecise but evocative summary of the unique and far-reaching features of this remarkable substance.

2. Model and methods

Several chemical mechanisms have been proposed for the THP pH oscillator [16–18,20,22,28], all of which involve autocatalysis by hydrogen ions to provide the isothermal rate nonlinearity necessary (at least cubic) to reproduce experimental oscillatory time traces. For this work, we have chosen to use the mechanism of Rábai & Hanazaki [20,29], described by the first seven reactions and equilibria in table 1, and appropriate for relatively low input concentrations of the reactants (∼mM). (We will introduce the role of reaction R8, which becomes important for higher input concentrations, in §3.1.)

Dynamical simulations were carried out within the CSTR paradigm [30]: i.e. a gradientless, continuous flow reacting system housed in a microcell, representing a rock pore, that is in thermal contact with its environment. The enthalpy balance includes all reaction enthalpy ΔH contributions, the heat transported by the flow with flow rate F, and the rate of heat lost to the environment, with coefficient L the thermal conductance of the microcell walls:

$$V\bar{C}\frac{\mathrm{d}T}{\mathrm{d}t} = V\sum_n(-\Delta H_i)r_i(T) + F\bar{C}(T_\mathrm{f} - T) + L(T_\mathrm{a} - T), \quad (2.1)$$

where the summation is over n temperature-dependent reaction rates $r_i(T)$. A mass balance for each reactant species has the form

$$V\frac{\mathrm{d}c_x}{\mathrm{d}t} = V\sum_p \delta r_i(T) + F(c_{x,\mathrm{f}} - c_x), \quad (2.2)$$

where c_x is concentration of reactant or intermediate x, the summation is over the p reaction rates that involve x, $c_{x,\mathrm{f}} = 0$ for intermediate species, $\delta = 1$ for intermediates that are produced and $\delta = -1$ for reactants and intermediates that are consumed. The rate coefficients k_i of the reaction rates r_i have Arrhenius temperature dependence:

$$k_i(T) = z_i \exp\left(\frac{-E_i}{\mathrm{RT}}\right).$$

Note that in §3.2, we will assume that the rate coefficients for RNA reactions also depend on pH. The symbols and quantities used here and henceforth are defined in table 2, where numerical values for the non-variable parameters are also given.

Table 1. Reactions involved in the THP thermo-pH oscillator.

low concentration oxidation with tetrathionate formation:	
$H_2O_2 + S_2O_3^- \rightleftharpoons HOS_2O_3^- + OH^-$	R1, $R1_r$
$H_2O_2 + HOS_2O_3^- \rightarrow 2HSO_3^- + H^+$	R2
$S_2O_3^{2-} + S_2O_3 \rightarrow S_4O_6^{2-}$	R3
$H_2O \rightleftharpoons H^+ + OH^-$	R4, $R4_r$
$H_2O_2 + HSO_3^- \rightarrow SO_4^{2-} + H_2O + H^+$	R5
$H_2O_2 + HSO_3^- + H^+ \rightarrow SO_4^{2-} + H_2O + 2H^+$	R5b
$HSO_3^- \rightleftharpoons H^+ + SO_3^{2-}$	R6, $R6_r$
$HOS_2O_3^- + H^+ \rightleftharpoons S_2O_3 + H_2O$	R7, $R7_r$
high concentration, deep oxidation with trithionate formation:	
$S_2O_3^{2-} + 2H_2O_2 \rightarrow \frac{1}{2}S_3O_6^{2-} + \frac{1}{2}SO_4^{2-} + 2H_2O$	R8

Using the kinetic data and reaction enthalpies in table 3, various selected values for the feed concentrations $c_{x,\mathrm{f}}$ and flow rate F, we integrated equations (2.1) and (2.2) from convenient initial conditions using a stiff integrator to obtain time series. We also monitored the linear stability of the steady-state solutions by computing the eigenvalues.

3. Results and discussion

Before we can use the THP oscillator to drive RNA replication, we need to develop an overall picture of its behaviour, so in §3.1, we present some relevant numerical analyses of the system in low and high feed concentration regimes. In §3.2, we evaluate the performance of an RNA replicating system under thermo-pH oscillatory drive.

3.1. Characterization of the THP oscillator

First, we computed solutions of equations (2.1) and (2.2), where the mass and enthalpy balances are taken for the reactants and intermediates of reactions and equilibria R1 to R7 in table 1.

The THP system exhibits regular and irregular pH oscillations when fed with low concentrations (∼mM) of reactants, for which thermal oscillations are negligible (refer forward to figure 6*a*). In figure 2, we localize the oscillations with respect to F by monitoring the stability of the steady-state solutions as F is varied. The pH declines as F is increased quasi-statically. The points marked X are Hopf bifurcations, where the real parts of a pair of complex conjugate eigenvalues become positive. Between the Hopf bifurcations the steady-state solutions are unstable and the stable solutions are oscillatory.

We selected three values of F within this oscillatory range and computed the corresponding time series. They are plotted in figure 3. We see that as the flow rate F is increased the oscillation period becomes longer, and the trace becomes more complex. Complex behaviour should be expected, as we are dealing with a high-dimensional dynamical system. (Chaotic and bursting dynamics have been recorded experimentally in this system [19,33].) At these low feed concentrations of reactants, the small specific reaction heat is absorbed by and lost to the system, which remains nearly isothermal.

Table 2. Nomenclature and constant numerical values. The numerical values of parameters that are varied within or between simulations are given in the figure captions.

symbol (units), definition	quantity	numerical value
c or $[\cdots]$ (M), concentration		
$\bar{C}$ (J K^{-1} l^{-1}), volumetric specific heat	$\bar{C}$	3400
E (kJ mol^{-1}), activation energy		
$E^{\ominus}$ (V), standard reduction potential		
F (μl s^{-1}), flow rate		
ΔH (kJ mol^{-1}), reaction enthalpy		
k (M^{-1} s^{-1} or s^{-1}), reaction rate constant		
L (mW K^{-1}), wall thermal conductance		
m, power-law exponent		
R (J mol^{-1} K^{-1}), gas constant		8.31447
T (K), temperature	T_a	283
	T_f	282
τ (s), oscillation period		
V (μl), reaction volume	V	10.0
X, X', RNA complementary single-strands		
XX', RNA duplex		
z (M^{-1} s^{-1} or s^{-1}), pre-exponential factor		
Z, intermediate RNA quadruplex		
subscripts		
a	of the ambient or wall temperature	
f	of the feed or flow	
x	of a reactant or intermediate species	
xz	of reaction R9	
zx	of reaction R10	

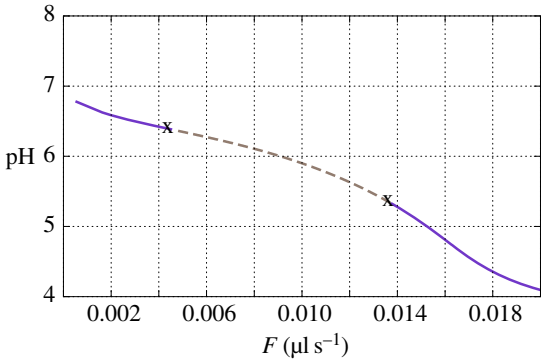

Figure 2. Bifurcation diagram with respect to variation of F for the THP oscillator in the isothermal regime. Parameters: $[H_2O_2]_f = 0.0135$ M, $[S_2O_3^{2-}]_f = 5.0$ mM, $[H^+]_f = 0.5$ mM, $[SO_3^{2-}]_f = 2.0$ mM, $L = 0.1$ mW K^{-1}. (Online version in colour.)

Table 3. Arrhenius parameters and reaction enthalpies for the THP reactions in table 1 [20,31,32].

reaction no.	E (kJ mol^{-1})	z (units)	ΔH (kJ mol^{-1})
R1	56.8	2.51×10^8 M^{-1} s^{-1}	20.8
$R1_r$	36.0	9.73×10^9 M^{-1} s^{-1}	−20.8
R2	92.2	1.92×10^{14} M^{-1} s^{-1}	−473.28
R3	61.2	4.42×10^{11} M^{-1} s^{-1}	−251.10
R4	55.84	4.55×10^6 s^{-1}[a]	55.84
$R4_r$	31.0	1.32×10^9 M^{-1} s^{-1}	55.84
R5	31.0	2.08×10^6 M^{-1} s^{-1}	−380.04
R5b	34.2	1.51×10^6 M^{-1} s^{-1}	−380.04
R6	75.1	3.95×10^{16} s^{-1}	49.3
$R6_r$	25.8	1.61×10^{15} M^{-1} s^{-1}[a]	−49.3
R7	25.8	4.82×10^7 M^{-1} s^{-1}	−41.3
$R7_r$	67.1	1.32×10^{10} s^{-1}	41.3
R8	68.12	1.63×10^{10} M^{-1} s^{-1}	572.2

[a] $z = z'[H_2O]$.

At higher feed concentrations, the system begins to feel the thermal effects, evidenced by the rapid development of a broad hysteresis in the steady-state solutions with respect to the flow rate F (figure 4).

In this case, the Hopf bifurcation at lower F, marked X, is preserved but the second Hopf bifurcation does not survive. Instead, the system develops multiplicity and the trend to lower pH with increasing F reverses. Following the peninsula of unstable solutions, we arrive at the point marked O, where all eigenvalues become negative. (As the system has dimensionality more than 2, stability need not change at a limit point.) In this X–O range, the solutions are oscillatory, and an example time series is shown in figure 5, where long periods of slow variation are interrupted by sharp 'kicks' in temperature and pH. Multiplicity of steady states has been observed experimentally in isothermal pH oscillators (e.g. [34]), but not, so far, in the thermo-pH regime.

We conjecture that thermo-pH cycles of such long period, approximately 5 h, were unlikely to have been useful in the RNA world, which operated on timescales of the order of minutes. But let us dwell on figure 5 a few moments, for it has heuristic value.

The change in form of the oscillations from figures 3 to 5 is striking. The isothermal pH oscillations in figure 3 occur simply because there is sufficient nonlinearity in the chemical rates to allow Hopf bifurcations—i.e. an effective reaction order of at least 3. Such power-law nonlinearities are weak compared with exponential nonlinearity, and the oscillations are usually gentle in form.

In figure 5, the transition to a thermokinetic regime has occurred. The power-law kinetics is completely dominated

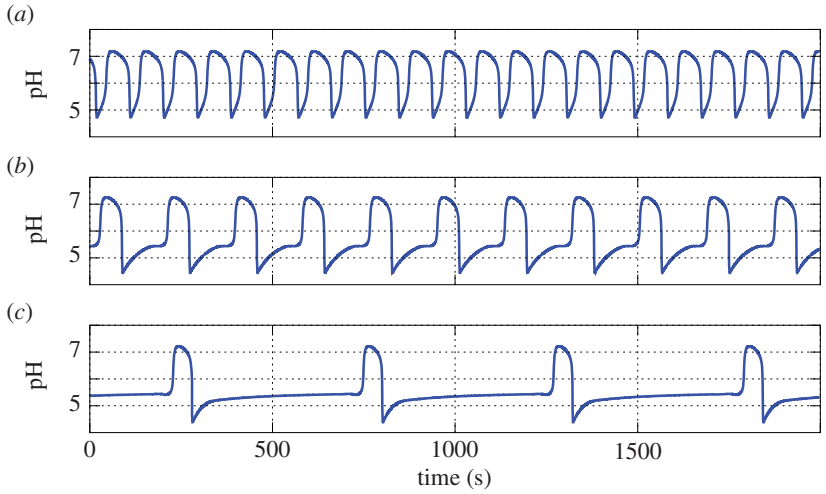

Figure 3. Time traces for the THP pH oscillator. (*a*) $F = 0.00661\ \mu l\ s^{-1}$, $\tau = 92$ s, (*b*) $F = 0.01061\ \mu l\ s^{-1}$, $\tau = 184$ s, (*c*) $F = 0.01261\ \mu l\ s^{-1}$, $\tau = 521$ s. Other parameters as given for figure 2. (Online version in colour.)

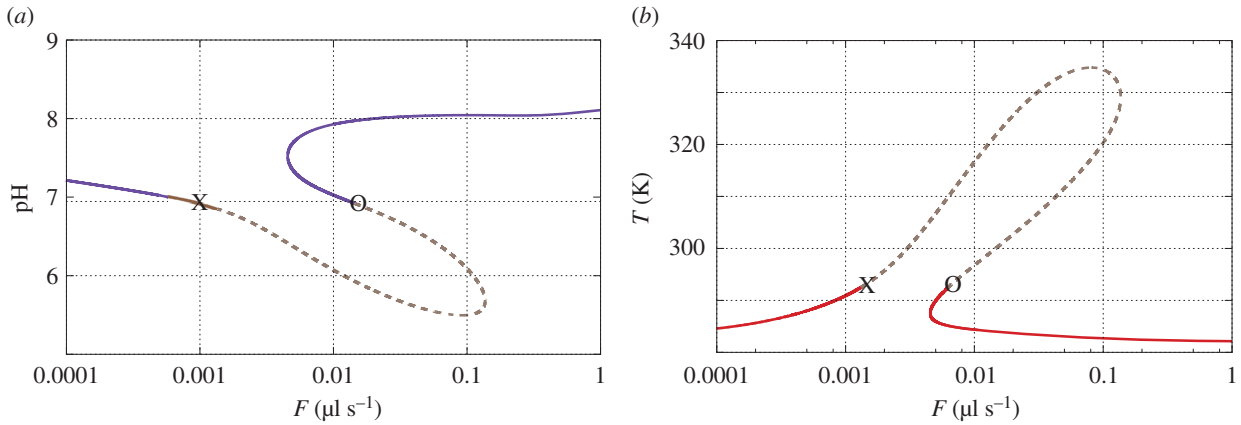

Figure 4. Bifurcation diagram with respect to variation of F for the THP oscillator in the thermokinetic regime, rendered in terms of the pH (*a*) and the temperature (*b*). Parameters: $[H_2O_2]_f = 0.054$ M, $[S_2O_3^{2-}]_f = 0.054$ M, $[H^+]_f = 0.5$ mM, $[SO_3^{2-}]_f = 2.0$ mM, $L = 0.1$ mW K^{-1}. (Online version in colour.)

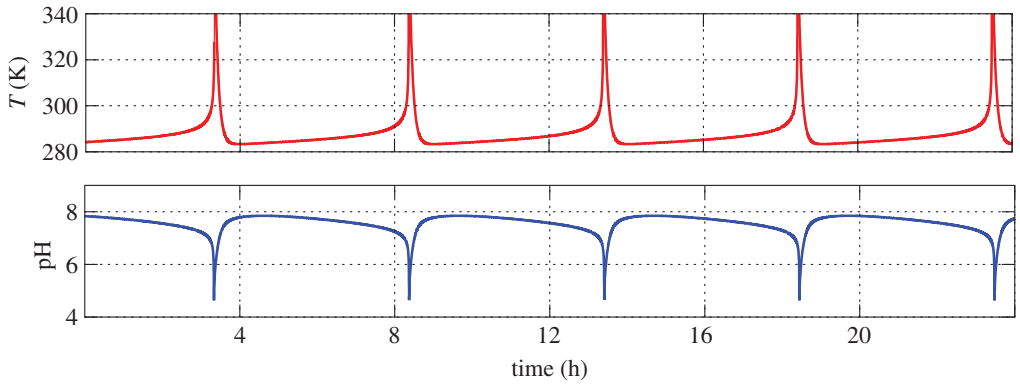

Figure 5. Time series for $F = 0.0026\ \mu l\ s^{-1}$. Other parameters as given for figure 4. (Online version in colour.)

by the exponential thermokinetics, giving rise to spiky relaxation oscillations over which energy accumulation and dissipation occur on different timescales, governed by the specific heat of the medium and the thermal conductance. For aqueous hydrogen peroxide solution, the specific heat is high, and the system barely heats up for a long time, even though heat is being released by reaction. This is because the liquid molecular structure can store large amounts of heat in quantized internal rotational modes and intermolecular vibrational potentials. When these modes become saturated, the heat is released in a great spike, which quickly subsides due to local depletion of reactant, and the relaxation oscillation cycle begins again. This is why one should expect to see violent spikes in a thermokinetic regime. Of course, one can choose parameters so the thermal oscillations are more sinusoidal in form (we will do this in §3.2), but there will always be a broad region of violent relaxation oscillations in a thermokinetic system, and almost none in a power-law system. This behaviour was teased out and elucidated using formal two-timing analysis in [35].

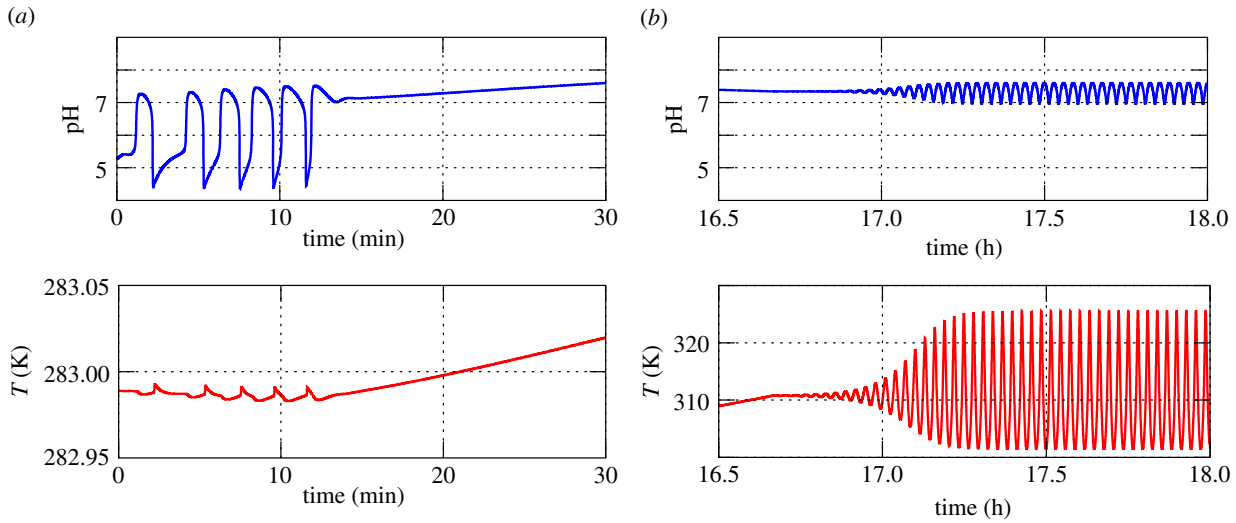

Figure 6. Under slow drift of parameters, the THP system shifts from (*a*) nearly isothermal pH oscillations, through a wide time range (not shown for convenience) where the pH drifts slowly up to around 8 then declines to around 7.2, to (*b*) the thermo-pH oscillatory regime. Values of feed parameters—initial: $F = 0.0106$ µl s^{-1}, $[H_2O_2]_f = 0.0135$ M, $[S_2O_3^{2-}]_f = 0.005$ M, final: $F = 0.430$ µl s^{-1}, $[H_2O_2]_f = 1.35$ M, $[S_2O_3^{2-}]_f = 0.9$ M. Parameters kept constant: $[H^+]_f = 0.5$ mM, $[SO_3^{2-}]_f = 2.0$ mM, $L = 2$ mW K^{-1}. (Online version in colour.)

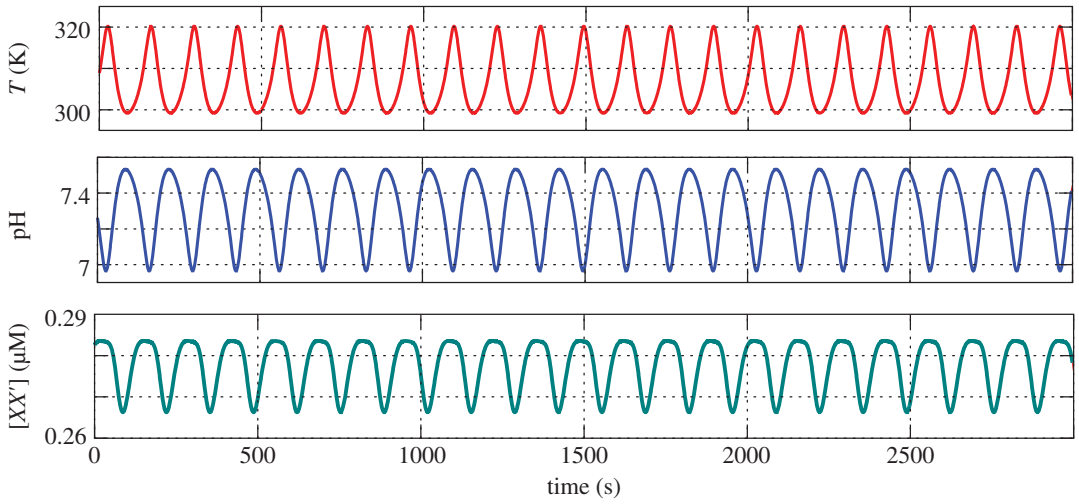

Figure 7. Time series for the THP system in the thermo-pH regime with reactions R9 and R10 included self-consistently, rendered in terms of the temperature, pH and concentration of double-stranded RNA. $F = 0.48$ µl s^{-1}, $[H_2O_2]_f = 1.35$ M, $[S_2O_3^{2-}]_f = 0.9$ M, $[H^+]_f = 0.0005$ M, $[SO_3^{2-}]_f = 0.0016$ M, $[X+X']_f = 500$ nM, $[XX']_f = 35$ nM, $L = 2$mW K^{-1}, $m_1 = m_2 = -1$, $\tau = 133.5$ s. (Online version in colour.)

The forms of the oscillations in figures 3 and 5 are strikingly similar to those in figs 6, 7 and 2 of Kovács & Rabái [29], and the bifurcation diagram of figure 4 suggests regions of bistability. The difference is that our simulations include the full thermal dynamics self-consistently (equations (2.1) and (2.2)), whereas theirs did not. We now have the capability to simulate thermo-kinetic dynamics and chemical power-law dynamics in the same simulation, which, as far as we know, is a first in the pH oscillator literature.

Experimental evidence [12–15] tells us that at higher feed concentrations than those used for figure 3, the highly exothermic, deep oxidation reaction R8 in table 1 takes over, with production of trithionate, and the kinetics are described by a simple second-order rate law. Therefore, we will not consider the regime exemplified in figure 5 further in this work, but file it away for possible future reference. A dramatic thermo-pH shake-up every 5 h or so possibly may have benefitted the RNA world in ways we cannot yet imagine.

It is not known how the switch to an R8 dominated mechanism occurs, probably because—as intimated earlier—the THP pH oscillator and the THP thermochemical oscillator were studied independently by researchers from different disciplines, but we have simulated a continuous transition from the low feed concentration, nearly isothermal regime to the high feed concentration, thermo-pH ocillatory regime as follows:

— we gave the feed parameters $[H_2O_2]_f$, $[S_2O_3^{2-}]_f$ and F small constant time dependences;
— we employed an additional time-dependent dummy parameter that was allowed to vary between 1 and 0 over a certain period to 'fade-out' the contributions of reactions R1, R1$_r$, R2, R3, R5, R5b, R7 and R7$_r$ in table 1;
— another time-dependent dummy parameter multiplied contributions from reaction R8 and was allowed to vary between 0 and 1 to 'fade-in' contributions from R8; and

— we integrated the system so that the 'fade-out' and 'fade-in' occurred over 8.3 h, allowed the evolution to continue with the slow parameter drift for a further 8.3 h, then continued the integration with constant parameters until 18 h. This result is visualized in figure 6.

In (a), the initial high amplitude pH and almost-zero amplitude thermal oscillations quickly damp out as the feed and dummy parameters are smoothly varied, until, much later, in (b) the system enters the thermo-pH regime, with the onset of pH and substantial thermal oscillations. The temperature range of (b) is compatible with current evidence that the temperature of the Palaeoarchaean ocean was $\lesssim 40^{\circ}$C [36].

Having identified and familiarized ourselves (somewhat) with these two regimes of the THP oscillator, we present an example for which it is used to drive RNA replication, to illustrate how it may have operated as an intrinsic periodic power source in the RNA world.

3.2. Enhancement of RNA replication

In our previous work [11], we showed that the THP thermochemical oscillator, with no pH dynamics, could drive replication of a 39-bp RNA duplex by complementary strand pairing in a continuous-flow system, using the following autocatalytic scheme:

$$X + X' + XX' \xrightarrow{k_{xz}} Z \qquad \text{R9}$$

and

$$Z \xrightarrow{k_{zx}} 2XX', \qquad \text{R10}$$

where X and X' represent RNA complementary single-strands, the RNA duplex XX' is the replicator and Z is an intermediate RNA quadruplex that decays to the duplex product.

It is thought that the RNA world may have developed in a slightly acid milieu [37]. However, there is no universal dependence of RNA reactive and conformational dynamics on pH, so for heuristic purposes in this work we assume that the rate coefficients have a power-law dependence on pH as

$$k_{xz} = z_{xz} \exp\left(\frac{E_{xz}}{\mathrm{RT}}\right)[\mathrm{H}^+]^{m_1} \qquad (3.1)$$

and

$$k_{zx} = z_{zx} \exp\left(\frac{E_{zx}}{\mathrm{RT}}\right)[\mathrm{H}^+]^{m_2}, \qquad (3.2)$$

and use the THP thermo-pH oscillator to drive replication of this RNA species, running two simulations: with $m_1 = m_2 = -1$ (pH-dependent case (a)), and with $m_1 = m_2 = 0$ (pH-independent case (b)). Values of the kinetic parameters and reaction enthalpies for R9 and R10 are given in table 4. (In a forthcoming work [38], we report THP oscillator simulations in which we have used experimentally determined pH dependences of the rates of ribozyme reactions.)

A time series for the pH-dependent case is shown in figure 7. Evidence from the literature indicates that the pH range of the signal, from 6.8 to 7.6, is reasonable for assisting thermal strand separation: e.g. Kao & Crothers [39] reported a melting transition for *E. coli* 5S rRNA between 10 and 40°C at a pH of 7.45, and that this transition was sharply dependent on pH between 7 and 8. We see from the time series that duplex concentration rises as pH falls and as temperature rises. This is expected: higher temperatures are needed to separate the intermediate quadruplex species into two newly replicated duplexes, and cooler temperatures at higher pH facilitate complementary strand pairing. The negative values of the exponents m_1 and m_2 in equations (3.1) and (3.2) imply that the reaction rates increase with a mean increase in pH, so let us quantify this increase.

Table 4. Arrhenius parameters and reaction enthalpies for reactions R9 and R10, from [11].

reaction no.	E (kJ mol^{-1})	z (units)	ΔH (kJ mol^{-1})
R9	−10.0	1.69×10^{12} M^{-1} s^{-1}	−260.14
R10	260.14	1.0×10^{32} s^{-1}	260.14

Table 5. Comparison of THP oscillator driven RNA replication for the pH-dependent case (*a*) and the pH-independent case (*b*).

case	m_1	m_2	$[XX']_{\mathrm{av}}$ (μM)	$[\dot{X}\dot{X}']_{\mathrm{av}}$ (pM s^{-1})	$\mathrm{pH}_{\mathrm{av}}$
(*a*)	−1	−1	0.2777	92.56	7.31
(*b*)	0	0	0.03494	11.65	7.20

The performance of the two cases is compared in table 5. We see that the average instantaneous concentration of double-stranded RNA, $[XX']_{\mathrm{av}}$, and the average production rate of double-stranded RNA, $[\dot{X}\dot{X}']_{\mathrm{av}}$, are higher by a factor of almost 7 for case (a) over case (b). For a replicating, evolving RNA world this effect could be significant:

— At given temperature, a higher rate of production of XX' implies that longer strands can be effectively replicated and separated. How much longer? We can write

$$E_{zx(a,h)} - E_{zx} = -\mathrm{RT} \ln\left(\frac{k_{zx(a)}[\mathrm{H}^+]_{(a)}^{-1}}{k_{zx(b)}}\right),$$

where $E_{zx(a,h)}$ is the hypothetical activation energy of the reaction under case (a) involving the putative longer strands. At 298 K, using data from tables 3 and 4, we find $E_{zx(a,h)} - E_{zx} = 41\,704.6$ J mol^{-1}. As a rough estimate, the activation energy per base pair is $E_{zx}/39$ bp ≈ 6670 J/(mol bp), thus the pH dependence of case (a) would allow for strands of up to 45 bp to replicate as efficiently as strands of 39 bp.

This lengthening of the RNA chain that can be replicated would be highly advantageous, in that there is considerably more scope for longer chains to evolve and develop and diversify enzyme activity, such as helicase and ligase functions that reduce the reliance of the RNA world on thermal cycling.

We also begin to perceive that the THP oscillator serves another, somewhat subtle, function in the RNA world: it is effectively preparing the RNA world for survival when hydrogen peroxide itself is no longer available in sufficient concentration to drive it thermally.

— Conversely, we can say that pH cycling would allow 39 bp strands to continue to replicate as the available concentration of hydrogen peroxide falls and the amplitude of the thermal oscillations becomes lower.

This can be viewed as another way in which the THP oscillator prepares the RNA world for a decline in the concentration of hydrogen peroxide.

We can now quantify, roughly, our assertion in the 'Introduction' section in the discussion of figure 1, that thiosulfate outcompetes RNA as a substrate for oxidation by hydrogen peroxide. This is achieved simply by a mass action argument: from the datafile for figure 7, the average concentration of thiosulfate is 4.53 mM and from table 5 that of RNA is 0.2777 μM for case (a). The oxidizable base of ribonucleotides is typically G (oxidized to 8-oxoG) [40], which has an average concentration of 0.0694 μM. Thus, we can deduce, as a rough estimate, that a hydrogen peroxide molecule is approximately $45\,030/0.0694 \approx 65\,000$ times more likely to encounter a thiosulfate ion than a G residue.

We ran time series for various other combinations of integer values for m_1 and m_2, but for none of these other cases was the performance improved. However, these results need not be taken too literally or narrowly. For one thing, the true pH dependence over the pH range can only be determined by experiment. What the results suggest more than anything is that an oscillatory pH drive allows the RNA system to access more degrees of freedom and gives it the flexibility potentially to adapt, self-optimize and run multiple operations simultaneously. Under constant pH, it cannot exhibit such versatility. In this sense, the RNA world under oscillatory drive resembles a truly living system.

4. Further discussions

4.1. Friend and foe

We reviewed in [11], the stability of RNA in a hydrogen peroxide milieu, and concluded that (i) RNA certainly may replicate and amplify faster than it is degraded, and (ii) hydrogen peroxide is an agent for mutation and therefore evolution. We believe that concern over its alleged toxicity in the current context is largely misplaced. Here, we offer the following additional insights:

— The notion that hydrogen peroxide is inimical to all life stems from its use as a disinfectant and its branding as one of the 'toxic' ROS (and, possibly, its misuse in criminal bomb-making exercises). The fact that ROS damage genetic material in cells and cause disease in humans is not relevant when considering the RNA world. A more nuanced view of its essential role in biology has emerged recently, as discussed in §1.
— To this day, some biological structures are highly resilient to hydrogen peroxide, e.g. macrophages [41] and some RNA sequences [42].
— Is hydrogen peroxide a strong oxidant, as sometimes claimed? Well no, actually, not always. Tables listing standard half-cell reduction potentials $E^{\ominus}$ would seem to provide definitive proof of its oxidizing strength, but although they are accurate a crucial piece of information is usually missing or buried in fine print on another page. From such tables, we glean that for the reduction half-reaction $H_2O_2 + 2H^+ + 2e^- \rightarrow 2H_2O$, $E^{\ominus} = 1.78\,V$, and that there are very few half-reactions that are more strongly oxidizing. What seems often to be overlooked is that *by definition* $E^{\ominus}$ for solutes in aqueous solution refers to a pH of 1. The plots of potential versus pH in figure 8 show that around biological pH hydrogen peroxide is a very much weaker oxidant (lower two lines), with a half-cell reduction potential of 1.2 V at pH = 7 for millimolal concentration. (The sign convention is reversed in the older literature, from which figure 8 was taken.) This compares with $E^{\ominus} = 1.23\,V$ for the reduction half-reaction $O_2 + 4H^+ + 4e^- \rightarrow 2H_2O$, and we survive and prosper (more or less) under a partial pressure of oxygen approximately 0.21 atm!
— So, under mild pH conditions, it is a relatively weak oxidant on its own. Usually it requires activation, e.g. by transition metal ions, to react.
— One could postulate some type of compartmentalization, such that the thermo THP oscillator in an 'outside' medium drives RNA reactions that are in thermal contact but mass isolated from it. Within the 'inner' RNA compartment, the pH-only THP oscillator may operate. Such compartmentalization may have occurred in the complicated structure of ancient hydrothermal rocky environments. In this context, we also note interesting findings that—contrary to common belief—hydrogen peroxide does not diffuse freely across plasma membranes [44,45].
— Under the action of the THP oscillator, RNA is exposed to high concentrations only intermittently, not constantly.

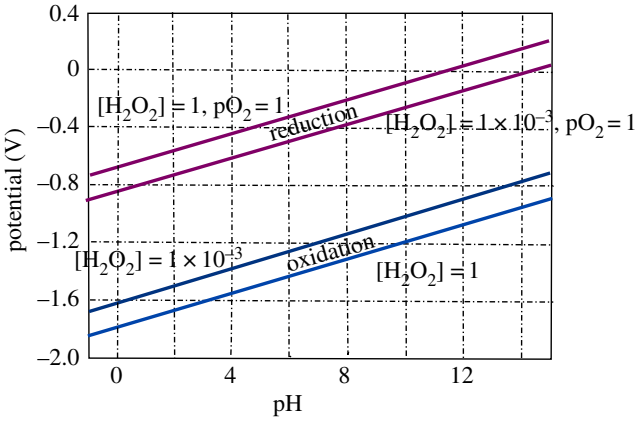

Figure 8. Potential–pH diagram for hydrgen peroxide–water solutions. Lower two lines are for the oxidizing half-reaction $2H_2O \rightarrow H_2O_2 + 2H^+ + 2e^-$. Upper two lines are for the reducing half-reaction $H_2O_2 \rightarrow O_2 + 2H^+ + 2e^-$. Solutes are in molal units, the gas pressure is in atm. Adapted from [43]. (Online version in colour.)

4.2. pH gradients and the proton motive force

The proton motive force is the physical manifestation of an electrochemical gradient of H^+ concentration and electrical potential due to charge separation, without which life, as we know it, could not exist. In cells, proton gradients occur across membranes and power processes such as photosynthesis, respiration and transport. But proton gradients existed in the RNA world before the evolution of cell membranes embedded with ATP synthase.

Lane *et al.* [46] make a strong case that the source of power for early life could not have been UV radiation or lightning, which destroy as much as they create, but must have been a continuing and replenishing source of chemical energy. They propose that life harnessed natural proton gradients around hydrothermal vents, remarking (justifiably, in our view) that

it is nearly impossible to see how life could have begun in the absence of proton gradients. The concept that primordial metabolic processes were driven by pH gradients between an acid external ocean and an alkaline hydrothermal fluid was developed further by Russell *et al.* [47], and by Barge *et al.* [48] in a fuel cell paradigm for abiogenesis.

We propose that the source both of this chemical energy *and* the proton gradients was hydrogen peroxide. In a spatially extended, bounded system the THP system is subject to diffusion and convection, and temporal oscillations manifest as travelling waves and patterns. (These have been studied experimentally in a THP system [49].) The gradients of a travelling thermo-pH wave provide a proton motive force that may have driven primitive metabolic processes in the non-cellular RNA world. Thus, the emergence of living systems need not be restricted to a narrow band around hydrothermal vents [47].

A spatial pH gradient of 2–3 pH units corresponds to a proton motive force of at least 118–177 mV from the concentration gradient alone, at 298 K. The low pH edge of the gradient is acidic, positively charged and oxidized relative to the high pH edge. This is sufficient to drive chemical processes that may have facilitated the RNA world—in other words, the beginnings of metabolism.

In time, primitive cells would have developed with the sophistication to use other sources of energy, such as methane, and the THP oscillator's role as a periodic power source faded out, but it had done its work of facilitating the emergence of living systems with the ability to maintain their own proton gradient drives across membranes.

— Again we see the role of the THP oscillator in preparing the systems it drives for continued existence without hydrogen peroxide.

We present this concept of a THP system-generated proton motive force purely as a hypothesis, leaving simulations of various scenarios as a series of potentially fruitful projects for students who enjoy playing with pde solvers and boundary conditions and high-performance computational ware, and, more urgently, for experimental investigations.

4.3. Occurrence of hydrogen peroxide in the solar system and beyond

In our earlier work [11], we discussed the evidence for production of hydrogen peroxide on the early Earth, and here we offer the following additional digest from the literature, expanding into space to introduce the idea that its presence could be an important biosignature in the search for life on other worlds.

— Saturn's 504 km diameter moon Enceladus is a geologically active body on which hydrogen peroxide may have been detected [50]. Enceladus is regarded as a potential habitat for life, because it is believed that a subsurface saltwater sea exists under the icy south pole [51].
— Hydrogen peroxide is present on Europa [52], where it is produced continuously by an incident flux of high-energy electrons from Jupiter's magnetosphere [53] and by high-energy ion bombardment [54]. Hand & Carlson [53] suggest that hydrogen peroxide and derived oxidants may play a critical role in maintaining biologically useful redox gradients in Europa's subsurface ocean [55,56].
— It occurs in the Mars atmosphere [57] and in Martian soils [58].
— Boduch *et al.* [59] surveyed results on high-energy ion bombardment of frozen carbon dioxide/water mixtures, which produced hydrogen peroxide and ozone, and discussed the results in the context of known facts about the icy moons of Jupiter, Saturn and Uranus. They found that oxidants formed at the surface by ion irradiation could diffuse and reach the putative subsurface ocean, where they could provide chemical energy for biological activities.
— Loeffler & Baragiola [60] studied the sublimation of water from solid H_2O_2/H_2O crystalline mixtures and found that in astronomical environments, such as icy satellites, where the mixture is shielded from radiolytic energetic fluxes, preferential evaporation of water may result in highly concentrated, possibly pure, hydrogen peroxide.
— Hydrogen peroxide has been detected in interstellar dust clouds [61].
— It is worth mentioning another interesting route for electrochemical generation of hydrogen peroxide on rocks [62], where electrical currents are set up by subsurface stresses.

5. Summary and conclusion

In summary, in this paper,

— We have proposed the hypothesis that spontaneous pH cycling enabled, firstly, replication of longer RNA species, and obtained simulation results in strong support (§3.2), and secondly, the harvesting of gradient energy by the RNA world. The pH gradient, or proton motive force, furnished by the THP oscillator may have facilitated development of primitive metabolism and liberated the RNA world from narrow regions around hydrothermal vents (§4.2).
— We have brought together for the first time, in the THP oscillator, a demonstration of simultaneous pH and thermochemical oscillations, by setting up and solving coupled dynamical mass and enthalpy balances for all the reactions involved (§§2 and 3.1). (This is a significant achievement in itself, because of the large size of the system (10–12 coupled, exponentially nonlinear, dynamical equations) and technical difficulties of numerical analysis, benchmarking and optimization of such a high-dimensional dynamical system.) As we remarked in the 'Introduction' section, the THP pH and thermochemical oscillators were separately studied for many years by two groups of researchers, which apparently remained entirely separate. We believe that this narrow, intra-disciplinary development meant that the versatility and potential of the THP reaction system was not appreciated until this work.
— Thus, we have created a new and powerful tool—the capability to include thermokinetic and chemical power-law dynamics of pH oscillators in the same simulation. This is the essential first step towards future spatio-temporal simulations of the RNA–THP oscillator system, in order, for example, to explore and develop our proposal (§4.2) that this pH cycling may have originally provided the ubiquitous proton motive force.

— We have included self-consistently the experimental thermokinetics and reaction enthalpies of an autocatalytic replicating RNA in the dynamical system for the THP oscillator, to study the effects of a dynamical pH environment on the replication, adopting a simple power-law dependence ($m_1 = m_2 = -1$) of the rate constants on hydrogen ion concentration, and found that replication occurs faster than for the pH-independent case. The significance of these simulations lies in the demonstration itself, that given the known importance of the pH environment in determining RNA behaviour and conformation, an oscillatory pH drive gives the RNA world much more freedom to develop varied functionalities. There is not much room for development of the RNA world under constant pH drive.
— Overall, we have generated results which we hope can constitute a recipe for definitive experiments, which could demonstrate that hydrogen peroxide may have powered the RNA world, and fill in some more pieces of the greatest puzzle in biology—the origin of life.

In conclusion, it is possible, perhaps even likely that the source of energy, thermal cycling and pH gradients that drove the RNA world was liquid hydrogen peroxide. We should not be surprised: it is the best of reactors, it is the worst of non-reactors, it is a reducing agent, it is an oxidizing agent, it is left-handed, it is right-handed, it was formed by light, it reacts in darkness, it selects, it mutates, it creates fitter life, it could help settle the RNA world into vesicles and initiate the ubiquitous dependence of all life on the proton motive force, it was *there*, on the Earth in the primordial epoch—in short, it is a superlative agent for the origin of life! Why would not Nature have made use of it in the primordial soup, and continue to use it in the intracellular soup?

Search for hydrogen peroxide on other Earth-like worlds, and eventually you will find conditions under which life may emerge, or have emerged.

Data accessibility. Data files from the computational simulations are available on request from the corresponding author. All information necessary to reproduce the results is given in the paper.

Authors' contributions. Both authors contributed to conception, design and intellectual development of the research, literature searches, and approved the final version of the paper. R.B. carried out mathematical modelling and simulations, interpreted the results and prepared the draft paper. J.B. contributed the initial design of figure 1, interpretation of simulation results and working up of the draft paper into final version.

Competing interests. We have no competing interests.

Funding. This work was funded by Australian Research Council Future Fellowship FT0991007 (R.B.).

Acknowledgements. We thank the anonymous referees for constructive and helpful comments and criticisms.

References

1. Ball R, Brindley J. Submitted. The life story of hydrogen peroxide III: chirality and physical effects at the dawn of life. *Orig. Life Evol. Biosph.*
2. Sies H. 2014 Role of metabolic H_2O_2 generation. *J. Biol. Chem.* **289**, 8735–8741. (doi:10.1074/jbc.R113.544635)
3. Schippers JHM, Nguyen HM, Lu D, Schmidt R, Mueller-Roeber B. 2012 ROS homeostasis during development: an evolutionary conserved strategy. *Cell. Mol. Life Sci.* **69**, 3245–3257. (doi:10.1007/s00018-012-1092-4)
4. Ślesak I, Ślesak H, Kruk J. 2012 Oxygen and hydrogen peroxide in the early evolution of life on earth: *in silico* comparative analysis of biochemical pathways. *Astrobiology* **12**, 775–784. (doi:10.1089/ast.2011.0704)
5. Bernhardt HS. 2012 The RNA world hypothesis: the worst theory of the early evolution of life (except for all the others). *Biol. Direct* **7**, 23. (doi:10.1186/1745-6150-7-23)
6. Orgel LE. 1992 Molecular replication. *Nature* **358**, 203–209. (doi:10.1038/358203a0)
7. Szostak JW. 2012 The eightfold path to non-enzymatic RNA replication. *J. Syst. Chem.* **3**, 14. (doi:10.1186/1759-2208-3-2)
8. Ivica N, Obermayer B, Campbell GW, Rajamani S, Gerland U, Chen IA. 2013 Paradox of dual roles in the RNA world: resolving the conflict between stable folding and templating ability. *J. Mol. Evol.* **77**, 55–73. (doi:10.1007/s00239-013-9584-x)
9. Mills DR, Peterson RL, Spiegelman S. 1967 An extracellular Darwinian experiment with a self-duplicating RNA molecule. *Proc. Natl Acad. Sci. USA* **58**, 217–224. (doi:10.1073/pnas.58.1.217)
10. Kreysing M, Keil L, Lanzmich S, Braun D. 2015 Heat flux across an open pore enables the continuous replication and selection of oligonucleotides towards increasing length. *Nat. Chem.* **7**, 203–208. (doi:10.1038/nchem.2155)
11. Ball R, Brindley J. 2014 Hydrogen peroxide thermochemical oscillator as driver for primordial RNA replication. *J. R. Soc. Interface* **11**, 20131052. (doi:10.1098/rsif.2013.1052)
12. Chang M, Schmitz RA. 1975 An experimental study of oscillatory states in a stirred reactor. *Chem. Eng. Sci.* **30**, 21–34. (doi:10.1016/0009-2509(75)85112-8)
13. Guha BK, Narsimham G, Agnew JB. 1975 An experimental study of transient behavior of an adiabatic continuous-flow stirred tank reactor. *Ind. Eng. Chem. Process Des. Dev.* **14**, 146–152. (doi:10.1021/i260054a009)
14. Lin KF, Wu LL. 1981 Performance of an adiabatic controlled cycled stirred tank reactor. *Chem. Eng. Sci.* **36**, 435–444. (doi:10.1016/0009-2509(81)85026-9)
15. Grau MD, Nougués JM, Puigjaner L. 2000 Batch and semibatch reactor performance for an exothermic reaction. *Chem. Eng. Process.* **39**, 141–148. (doi:10.1016/S0255-2701(99)00015-X)
16. Orbán M, Epstein IR. 1987 Chemical oscillators in group VIA: the copper(II)-catalyzed reaction between hydrogen peroxide and thiosulfate ion. *J. Am. Chem. Soc.* **109**, 101–106. (doi:10.1021/ja00235a017)
17. Kurin-Csörgei K, Orbán M, Rábai G, Epstein IR. 1996 Model for the oscillatory reaction between hydrogen peroxide and thiosulfate catalysed by copper(II) ions. *J. Chem. Soc. Farad. Trans.* **92**, 2851–2855. (doi:10.1039/ft9969202851)
18. Gao Q, Wang Y, Wang G, Zhang S, Zang Y, Zhao X. 1997 Nonlinear chemical reaction between $Na_2S_2O_3$ and peroxide compound. *Sci. China B* **40**, 152–160. (doi:10.1007/BF02876406)
19. Rábai G, Hanazaki I. 1999 Chaotic pH oscillations in the hydrogen peroxide–thiosulfate–sulfite flow system. *J. Phys. Chem. A* **103**, 7268–7273. (doi:10.1021/jp991600r)
20. Rábai G, Hanazaki I. 1999 Temperature compensation in the oscillatory hydrogen peroxide–thiosulfate–sulfite flow system. *Chem. Commun* **1999**, 1965–1966. (doi:10.1039/a906598i)
21. Yuan L, Gao Q, Zhao Y, Tang X, Epstein IR. 2010 Temperature-induced bifurcations in the Cu(II)-catalysed and catalyst-free hydrogen peroxide–thiosulfate oscillating reaction. *J. Phys. Chem. A* **114**, 7014–7020. (doi:10.1021/jp102010k)
22. Lu Y, Gao Q, Xu L, Zhao Y, Epstein IR. 2010 Oxygen–sulfur species distribution and kinetic analysis in the hydrogen peroxide–thiosulfate system. *Inorg. Chem.* **49**, 6026–6034. (doi:10.1021/ic100573a)
23. Pešek O, Schreiberová L, Schreiber I. 2011 Dynamical regimes of a pH-oscillator operated in two mass-coupled flow-through reactors. *Phys.*

Chem. Chem. Phys. **13**, 9849–9856. (doi:10.1039/c1cp20125e)

24. Gray P, Scott SK. 1990 *Chemical oscillations and instabilities: non-linear chemical kinetics*. Oxford, UK: Clarendon Press.
25. Liedl T, Simmel FC. 2005 Switching the conformation of a DNA molecule with a chemical oscillator. *Nano Lett*. **5**, 1894–1898. (doi:10.1021/nl051180j)
26. Liedl T, Olapinski M, Simmel FC. 2006 A surface-bound DNA switch driven by a chemical oscillator. *Angew. Chem. Int. Ed*. **45**, 5007–5010. (doi:10.1002/anie.200600353)
27. Qi X-J, Lu C-H, Liu X, Shimron S, Yang H-H, Willner I. 2013 Autonomous control of interfacial electron transfer and the activation of DNA machines by an oscillatory pH system. *Nano Lett*. **13**, 4920–4924. (doi:10.1021/nl402873y)
28. Wayland Rushing C, Thompson RC, Gao Q. 2000 General model for the nonlinear pH dynamics in the oxidation of sulfur(-II) species. *J. Phys. Chem. A* **104**, 11 561–11 565. (doi:10.1021/jp0023314).
29. Kovács K, Rábai G. 2002 Temperature compensation in pH oscillators. *Phys. Chem. Chem. Phys*. **4**, 5265–5269. (doi:10.1039/b206497a).
30. Denbigh KG. 1984 *Chemical reactor theory: an introduction*, 3rd edn. Cambridge, UK: Cambridge University Press.
31. Goldberg RN, Parker VB. 1985 Thermodynamics of solution of SO_2(g) in water and of aqueous sulfur dioxide solutions. *J. Res. Natl Bur. Stand.* **90**, 341–358. (doi:10.6028/jres.090.024)
32. Williamson MA, Rimstidt JD. 1992 Correlation between structure and thermodynamic properties of aqueous sulfur species. *Geochim. Cosmochim. Acta* **56**, 3867–3880. (doi:10.1016/0016-7037(92)90002-Z)
33. Bakeš D, Schreiberová L, Schreiber I, Hauser MJB. 2008 Mixed-mode oscillations in a homogeneous pH-oscillatory chemical reaction system. *Chaos* **18**, 015102. (doi:10.1063/1.2779857)
34. Kovács K, McIlwaine RE, Scott SK, Taylor AF. 2007 pH oscillations and bistability in the methylene glycol–sulfite–gluconolactone reaction. *Phys. Chem. Chem. Phys*. **9**, 3711–3716. (doi:10.1039/B704407K)
35. Ball R. 2011 Thermal relaxation oscillations in liquid organic peroxides. *Int. J. Energ. Mater. Chem. Propulsion* **10**, 523–540. (doi:10.1615/IntJEnergeticMaterialsChemProp.2012005092)
36. Hren MT, Tice MM, Chamberlain CP. 2009 Oxygen and hydrogen isotope evidence for a temperate climate 3.42 billion years ago. *Nature* **462**, 205–208. (doi:10.1038/nature08518)
37. Bernhardt HS, Tate WP, Warren P. 2012 Primordial soup or vinaigrette: did the RNA world evolve at acidic pH? *Biol. Direct* **7**, 4. (doi:10.1186/1745-6150-7-4)
38. Ball R, Brindley J. 2015 Thiosulfate–hydrogen peroxide redox oscillator as pH driver for ribozyme activity in the RNA world. *Orig. Life Evol. Biosph.* (doi:10.1101/020693)
39. Kao T, Crothers DM. 1980 A proton-coupled conformational switch of *Escherichia coli* 5S ribosomal RNA. *Proc. Natl Acad. Sci. USA* **77**, 3360–3364. (doi:10.1073/pnas.77.6.3360)
40. Wurtmann EJ, Wolin SL. 2009 RNA under attack: cellular handling of RNA damage. *Crit. Rev. Biochem. Mol. Biol*. **44**, 34–39. (doi:10.1080/10409230802594043)
41. de la Haba C, Palacio JR, Martinez P, Morros A. 2013 Effect of oxidative stress on plasma membrane fluidity of THP-1 induced macrophages. *Biochim. Biophys. Acta Biomembr*. **1828**, 357–364. (doi:10.1016/j.bbamem.2012.08.013)
42. Altuvia S, Weinstein-Fischer D, Zhang A, Postow L, Storz G. 1997 A small, stable RNA induced by oxidative stress: role as a pleiotropic regulator and antimutator. *Cell* **90**, 45–53. (doi:10.1016/S0092-8674(00)80312-8)
43. Schumb WC, Satterfield CN, Wentworth RL. 1954 *Hydrogen peroxide*, p. 233. Technical Report 44, Part Three. Cambridge, MA: Massachusetts Institute of Technology.
44. Antunes F, Cadenas E. 2000 Estimation of H_2O_2 gradients across biomembranes. *FEBS Lett*. **475**, 121–126. (doi:10.1016/S0014-5793(00)01638-0)
45. Branco MR, Marinho HS, Cyrne L, Antunes F. 2004 Decrease of H_2O_2 plasma membrane permeability during adaptation to H_2O_2 in *Saccharomyces cerevisiae*. *J. Biol. Chem*. **279**, 6501–6506. (doi:10.1074/jbc.M311818200)
46. Lane N, Allen JF, Martin W. 2010 How did LUCA make a living? Chemiosmosis in the origin of life. *BioEssays* **32**, 271–280. (doi:10.1002/bies.200900131)
47. Russell MJ *et al.* 2014 The drive to life on wet and icy worlds. *Astrobiology* **14**, 308–343. (doi:10.1089/ast.2013.1110)
48. Barge LM *et al.* 2014 The fuel cell model of abiogenesis: a new approach to origin-of-life simulations. *Astrobiology* **14**, 254. (doi:10.1089/ast.2014.1140)
49. Gao Q, An Y, Wang J. 2004 A transition from propagating fronts to target patterns in the hydrogen peroxide–sulfite–thiosulfate medium. *Phys. Chem. Chem. Phys*. **6**, 5389–5395. (doi:10.1039/b412219d)
50. Newman SF, Buratti BJ, Jaumann R. 2007 Hydrogen peroxide on Enceladus. *Astrophys. J*. **670**, L143–L146. (doi:10.1086/524403)
51. Spencer JR, Nimmo F. 2013 Enceladus: an active ice world in the Saturn system. *Annu. Rev. Earth Planet. Sci*. **42**, 693–717. (doi:10.1146/annurev-earth-050212-124025)
52. Carlson RW *et al.* 1999 Hydrogen peroxide on the surface of Europa. *Science* **283**, 2062–2064. (doi:10.1126/science.283.5410.2062)
53. Hand KP, Carlson RW. 2011 H_2O_2 production by high-energy electrons on icy satellites as a function of surface temperature and electron flux. *Icarus* **215**, 226233. (doi:10.1016/j.icarus.2011.06.031)
54. Loeffler MJ, Raut U, Vidal RA, Baragiola RA, Carlson RW. 2006 Synthesis of hydrogen peroxide in water ice by ion irradiation. *Icarus* **180**, 265–273. (doi:10.1016/j.icarus.2005.08.001)
55. Chyba CF, Phillips CB. 2001 Possible ecosystems and the search for life on Europa. *Proc. Natl Acad. Sci. USA* **98**, 801–804. (doi:10.1073/pnas.98.3.801)
56. Hand KP, Carlson RW, Chyba CF. 2007 Energy, chemical disequilibrium, and geological constraints on Europa. *Astrobiology* **7**, 1006–1022. (doi:10.1089/ast.2007.0156)
57. Clancy RT, Sandor BJ, Moriarty-Schieven GH. 1975 A measurement of the 362 GHz absorption line of Mars atmospheric H_2O_2. *Icarus* **168**, 116–121. (doi:10.1016/j.icarus.2003.12.003)
58. Hurowitz JA, Tosca NJ, McLennan SM, Schoonen MAA. 2007 Production of hydrogen peroxide in Martian and lunar soils. *Earth Planet. Sci. Lett*. **255**, 41–52. (doi:10.1016/j.epsl.2006.12.004)
59. Boduch P *et al.* 2011 Production of oxidants by ion bombardment of icy moons in the outer solar system. *Adv. Astronomy* **2011**, 1–10. (doi:10.1155/2011/327641)
60. Loeffler MJ, Baragiola RA. 2011 Isothermal decomposition of hydrogen peroxide dihydrate. *J. Phys. Chem. A* **115**, 5324–5328. (doi:10.1021/jp200188b)
61. Bergman P, Parise B, Liseau R, Larsson B, Olofsson H, Menten KM, Güsten R. 2011 Detection of interstellar hydrogen peroxide. *Astron. Astrophys.* **531**, L8. (doi:10.1051/0004-6361/201117170)
62. Balk M, Bose M, Ertem G, Rogoff DA, Rothschild LJ, Freund FT. 2009 Oxidation of water to hydrogen peroxide at the rock–water interface due to stress-activated electric currents in rocks. *Earth Planet. Sci. Lett*. **283**, 87–92. (doi:10.1016/j.epsl.2009.03.044)